

Parametrization of the Tkatchenko-Scheffler dispersion correction scheme for popular exchange-correlation density functionals: effect on the description of liquid water

Miguel A. Caro^{1,2,*}

¹*Department of Electrical Engineering and Automation, Aalto University, Espoo, Finland*

²*COMP Centre of Excellence in Computational Nanoscience,
Department of Applied Physics, Aalto University, Espoo, Finland*

(Dated: January 15, 2018)

We present a list of optimized damping range parameters s_R to be used with the Tkatchenko-Scheffler van der Waals dispersion-correction scheme [Phys. Rev. Lett. 102, 073005 (2009)]. The optimal s_R are obtained for seven popular generalized-gradient approximation exchange-correlation density functionals: PBE, RPBE, revPBE, PBEsol, BLYP, AM05 and PW91. The optimization is carried out in the standard way by minimizing the mean absolute error of the S22 test set, where the reference interaction energies are taken from coupled-cluster calculations. With the optimized range parameters, we assess the impact of van der Waals corrections on the ability of these functionals to accurately describe structural and thermodynamic properties of liquid water: radial distribution functions, self-diffusion coefficients and standard molar entropies.

I. INTRODUCTION

The Tkatchenko-Scheffler (TS) method has emerged in recent years as one of the most popular dispersion-correction schemes in density functional theory (DFT) calculations [1]. The reason is that TS is a post-processing scheme, and can therefore be applied on top of DFT electron densities without significantly adding to the overall execution time of the different algorithms, where by far the most expensive part corresponds to the self-consistent calculation of the Kohn-Sham orbitals. It was shown by Marom *et al.* [2] that TS performs better than similar approaches for a wide variety of weakly interacting molecular systems.

The TS approach involves the optimization of an adjustable parameter, s_R , which determines the range at which the dispersion interactions begin to become important. The value of s_R depends on the intrinsic ability of the underlying exchange-correlation (XC) density functional to correctly describe van der Waals interactions. An optimal value of s_R is therefore functional-dependent. Tkatchenko and Scheffler originally optimized s_R [1] for the PBE functional [3] by minimizing the error in the interaction energies predicted with the PBE+TS approach compared with highly accurate coupled-cluster calculations [CCSD(T)] of the S22 test set by Jurečka *et al.* [4]. They obtained $s_R = 0.94$. Later on, Marom *et al.* optimized s_R for a number of hybrids and meta-generalized-gradient approximation (meta-GGA) XC functionals [2]. Agrawal *et al.* carried out follow-up work on the performance of TS corrections for hybrid functionals, including the role of the range-separation screening parameter, finding it to have little correlation with the optimization of s_R [5]. However, optimal s_R have not yet been estimated for many popular GGA functionals, which are routinely used preferentially over more advanced func-

tionals because of computational advantages. s_R is not transferable across XC functionals, and using for instance the PBE value with a different GGA may lead to unacceptable errors in the calculated dispersion corrections.

II. OPTIMIZATION OF s_R FOR SEVERAL XC FUNCTIONALS

In this paper we optimize s_R for some of the GGAs most widely used across the computational chemistry and physics communities: PBE (for benchmark with previous results), RPBE [6], revPBE [7], PBEsol [8], BLYP [9–11], AM05 [12] and PW91 [13]. We use the GPAW DFT suite [14] in conjunction with the Atomic Simulation Environment (ASE) [15], which offer an extremely flexible Python-based environment to carry out the present calculations (a sample Python script is presented at the end of this paper that allows to optimize s_R for any XC functional available from the LibXC library [16] and compatible with GPAW). We used the GPAW grid mode with 0.18 Å spacing and PAW potentials [17, 18]. We generated the PAW setups for the PBEsol, BLYP, AM05 and PW91 functionals using the GPAW setup generation tool. The DFT calculations were carried out in fixed boundary conditions within orthogonal boxes where at least 4 Å of vacuum was allowed between the atoms and the box boundaries.

The interaction energies are defined as the difference between the total energy of the interacting system (1+2) and the sum of the energies of each of the two isolated molecules (1 and 2):

$$E_i^{\text{int}} = E_i^{1+2} - E_i^1 - E_i^2, \quad (1)$$

where i labels each of the 22 molecular systems in the S22 set. The mean absolute error (MAE) and mean signed difference (MSD) between the interaction energies calculated with GPAW and those from the CCSD(T) S22 test set computed for each XC functional over a wide range of

* mcaroba@gmail.com

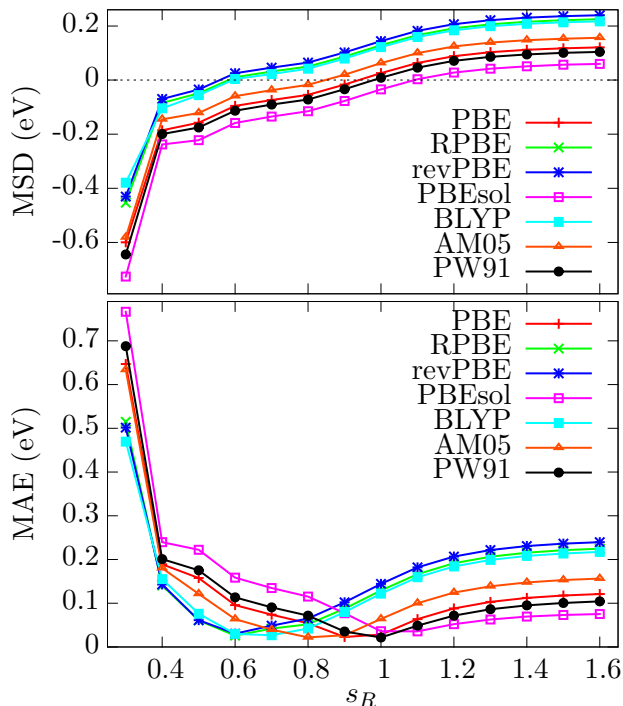


FIG. 1. Mean signed difference (MSD) and mean absolute error (MAE) of the TS method applied to different GGAs over a wide range of s_R values.

TABLE I. Optimal s_R fitted for each XC functional (resolved to nearest 0.005) and MAE calculated for the S22 test set. The calculations for each functional were run at the optimal value of s_R for that functional.

XC functional	s_R	MAE (meV)
PBE	0.940	16
RPBE	0.590	26
revPBE	0.585	29
PBEsol	1.055	30
BLYP	0.625	25
AM05	0.840	15
PW91	0.965	20

s_R values are shown in Fig. 1. One can observe the same overall trends regardless of the GGA used: the error increases rapidly as the value of s_R is reduced and slowly as it is increased. It can also be observed how the MAE for each functional has its minimum at a different position, emphasizing the fact that s_R values are not transferable across XC functionals and must be carefully optimized on an individual basis.

Figure 2 shows a detailed view of MSD and MAE in the regions where they are zero and minimum, respectively. Table I summarizes the optimal s_R parameter obtained for each XC functional studied and the MAE computed at said value of s_R . We obtain the same value for PBE as has been previously reported [1, 2]. As discussed by

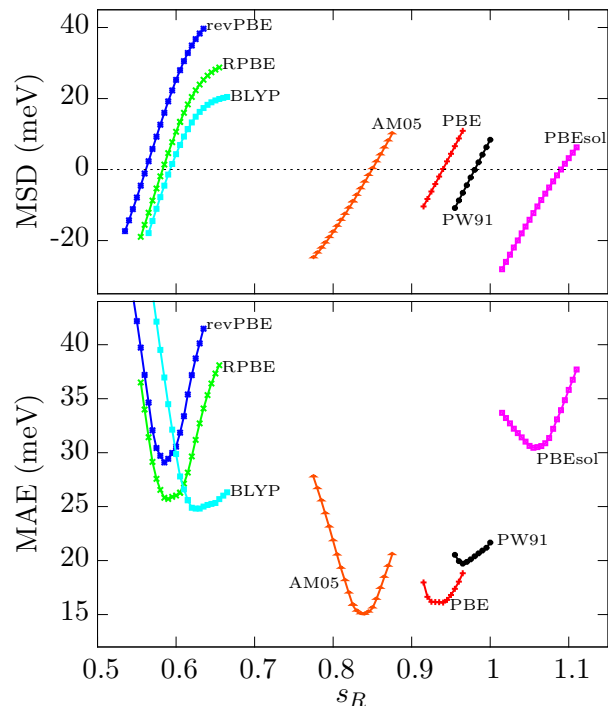


FIG. 2. Fine detail of Fig. 1 in the region where the errors are minimized.

Marom *et al.* [2], a low optimal s_R indicates that the underlying XC functional does a poor job at handling dispersion interactions on its own. From Fig. 2 and Table I we observe how revPBE, RPBE and BLYP cluster around the low s_R region, while AM05, PBE and PW91 cluster at intermediate values and PBEsol lies slightly beyond them. We also observe that AM05 and PBE see their MAE reduced to a very small value (~ 15 meV) with the inclusion of TS dispersion corrections, while revPBE and PBEsol retain larger errors of up to 30 meV even with the optimal s_R .

To get deeper insight into the different contributions to the overall errors, Fig. 3 shows the signed errors (SD) for each molecule in the S22 set and each functional, where the TS corrections are computed at the optimal s_R value for each XC functional. Note from the figure that the description of dispersion is not at all homogeneous across molecules. For instance, PBEsol+TS, which performs worst overall, does a very good job at describing many of the benzene-containing systems. We also note how several functionals give almost identical results to each other, for instance PW91 and PBE show almost identical curves. The same is true for RPBE and revPBE.

Based on these observations, the possibility to re-optimize s_R for a very specific problem by fitting to a more suitable test set remains viable. For instance, if one is interested in achieving an accurate description of a protein, s_R could be optimized to describe the dispersion interactions between a set containing different aminoacids and small organic molecules. The Python script in the Appendix automatizes the calculation of dispersion er-

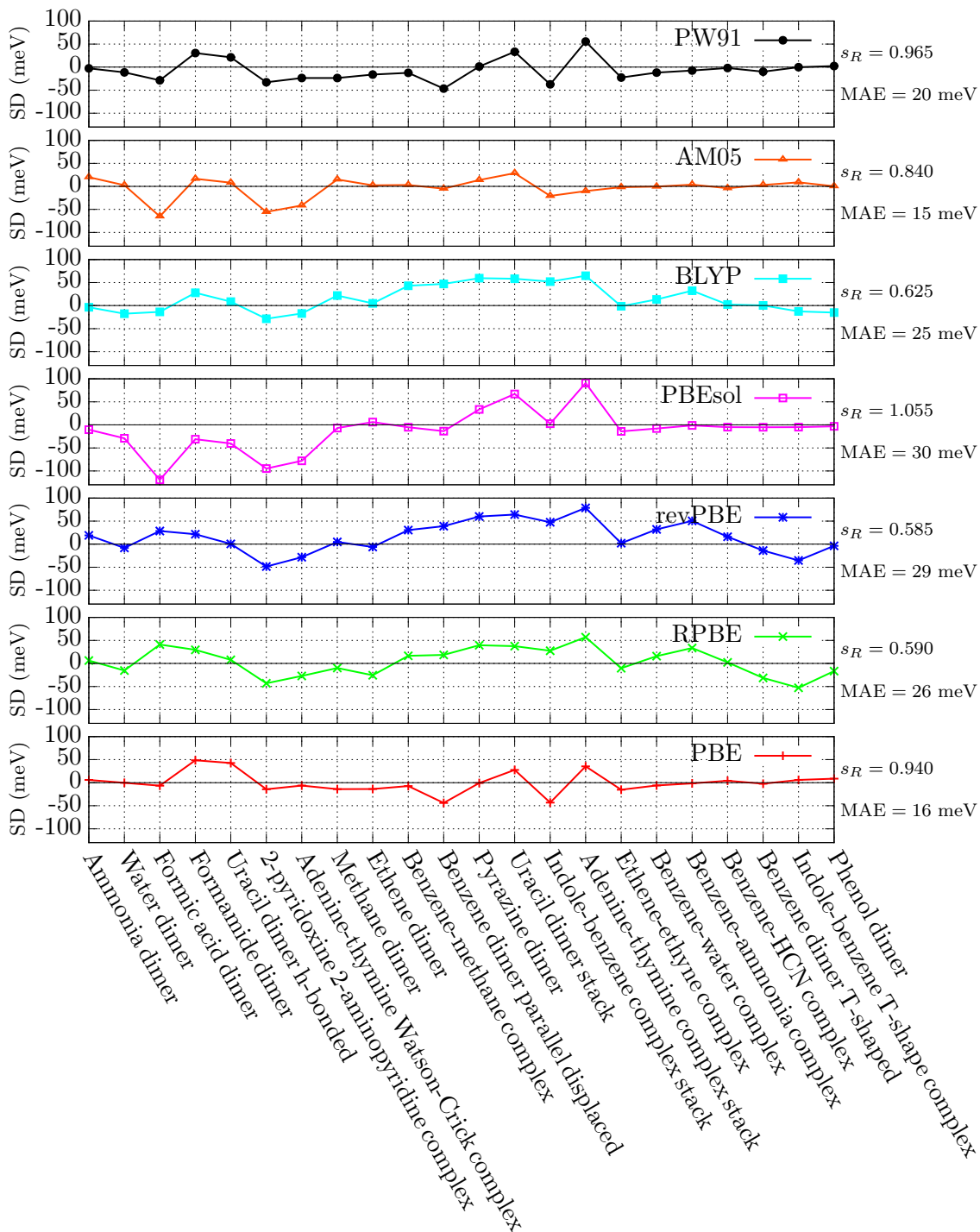


FIG. 3. Performance of the DFT+TS scheme for different GGA XC functionals, evaluated at each functional’s optimal s_R value for all and each of the molecular systems present in the S22 set.

rors presented in this paper, and can be used to optimize s_R for a different XC functional or test set (note that one needs to generate the corresponding PAW setups needed by GPAW beforehand if they are not installed by default).

III. APPLICATION OF DISPERSION CORRECTIONS TO DESCRIBE LIQUID WATER

To test the possible improvement over the underlying functionals brought about by the inclusion of dispersion corrections, we looked at molecular dynamics (MD) simulations of liquid water. A more exhaustive assessment

of the ability of DFT to correctly describe the properties of water is available from the recent excellent review by Gillan, Alfè and Michaelides [19]; here we are more concerned with identifying systematic improvements introduced by TS dispersion corrections. A detailed study along the same lines was conducted for the BLYP, PBE and revPBE functionals [20], although hydrogen nuclei were replaced by deuterium nuclei in that study. This has the observed effect of decreasing the self-diffusion constant of the liquid. In this study, the performance of the different GGAs for predicting structural and thermodynamic properties of water at ambient conditions (300 K) and experimental density (1 g/cm³) was studied with and without TS corrections. The properties that we looked at are: self-diffusion coefficient, radial distribution functions and standard molar entropy. We used periodic supercells containing 100 water molecules, pre-equilibrated with a classical potential and the Gromacs code [21]. We used the SPCE water model [22] (allowing for vibrations of the O-H intramolecular bonds) with the OPLS force field [23]. After this, 35 ps of *ab initio* MD (AIMD) followed. The AIMD part was performed with the plane-wave based DFT code VASP [24]. Since PAW potentials for VASP are only supplied for the PBE and LDA functionals, we carried out the AIMD using PBE PAW potentials for all the GGAs studied here. We used 0.5 fs as time step to correctly resolve hydrogen vibrations, and set the kinetic energy cutoff for the plane-wave basis set to 300 eV. The first 15 ps of dynamics for each simulation were discarded and the last 20 ps were analyzed with our own implementation [25, 26] of the 2PT method [27–29], DoSPT [30]. Unfortunately, we could not compute the AM05 values due to convergence problems in the MD runs. The values for all the other GGAs tested and reference experimental and classical MD values are given in Table II. Radial distribution functions are shown in Fig. 4 and detailed information regarding RDF peak positions is given in Table III.

In Ref. [19], uncorrected RPBE was observed to offer the best description of liquid water among the tested GGAs. Here, we observe the same behavior for RPBE but obtain best results in all the categories, including entropy, which was not surveyed in Ref. [19], for BLYP. The main difference between the sources quoted in Ref. [19] and this work is that all MD here were carried out with regular hydrogen nuclei (protium) rather than deuterium. We also ran all the simulations at the experimental density. Heavy water has a lower self-diffusion constant than regular water, and a quick test that we ran with the classical potential we employed for pre-equilibration (SPCE+OPLS) showed that the self-diffusion constant decreases by 40% when using deuterium nuclei instead of protium nuclei.

The revPBE functional shows very similar performance to the related RPBE functional. Surprisingly, the inclusion of TS dispersion corrections worsens the agreement with experiment for both of those functionals and BLYP, while it improves it for the others. PBEsol emerges as the

TABLE II. Standard molar entropies S_0 and self-diffusion coefficients D calculated for different GGAs with and without TS dispersion corrections at $T = 300$ K. Experimental and classical MD results are shown for comparison.

XC functional	D (10^{-9} m ² /s)	S_0 (J/mol/K)
PBE	0.57	43.2
PBE+TS	1.09	47.8
RPBE	1.61	54.4
RPBE+TS	1.09	49.1
revPBE	1.28	51.5
revPBE+TS	0.66	45.5
PBEsol	0.40	39.1
PBEsol+TS	0.49	40.8
BLYP	2.16	58.0
BLYP+TS	1.59	54.7
PW91	0.64	42.8
PW91+TS	0.92	45.0
OPLS+SPCE (rigid)	2.72	58.8
OPLS+SPCE (flexible)	1.54	53.3
Experiment	2.41 ^a	69.92 ^b

^a From Ref. [31].

^b From Ref. [32] at $T = 298$ K.

absolute loser in this comparison. The bad performance of PBEsol does not only affect the quantitative description of the properties of liquid water, but it also gives a qualitatively bad behavior of the water molecules during the MD. We observed significant spontaneous hydroxyl and hydronium ion formation with PBEsol: 4% of the oxygens were observed to be part of either a hydroxyl or a hydronium group at any time of the dynamics. This can be graphically observed as the lack of a clear minimum in the O-H radial distribution function in Fig. 4. Therefore, we conclude that the PBEsol functional should be avoided for any simulation that involves water molecules, such as simulations of solid/water interfaces, in order to prevent unphysical results.

The extremely popular PBE benefits from dispersion corrections by improved description of all the studied properties. However, the water overstructuring typical of the PBE functional cannot be completely suppressed with the inclusion of van der Waals corrections. A popular strategy, often found in the literature to tackle this issue, is to perform MD with PBE at high temperature. The also very popular BLYP functional offers by far the best description of water, in all the categories, in the absence of dispersion corrections. When adding TS corrections the description is slightly worsened, in particular the value of the self-diffusion coefficient. Unfortunately, BLYP is known to offer poor description of metallic systems [34], which may limit its wider applicability.

All the functionals underestimate standard molar entropies by large factors, which vary between a best-case scenario of 17% (BLYP) and worst-case scenario of 44%

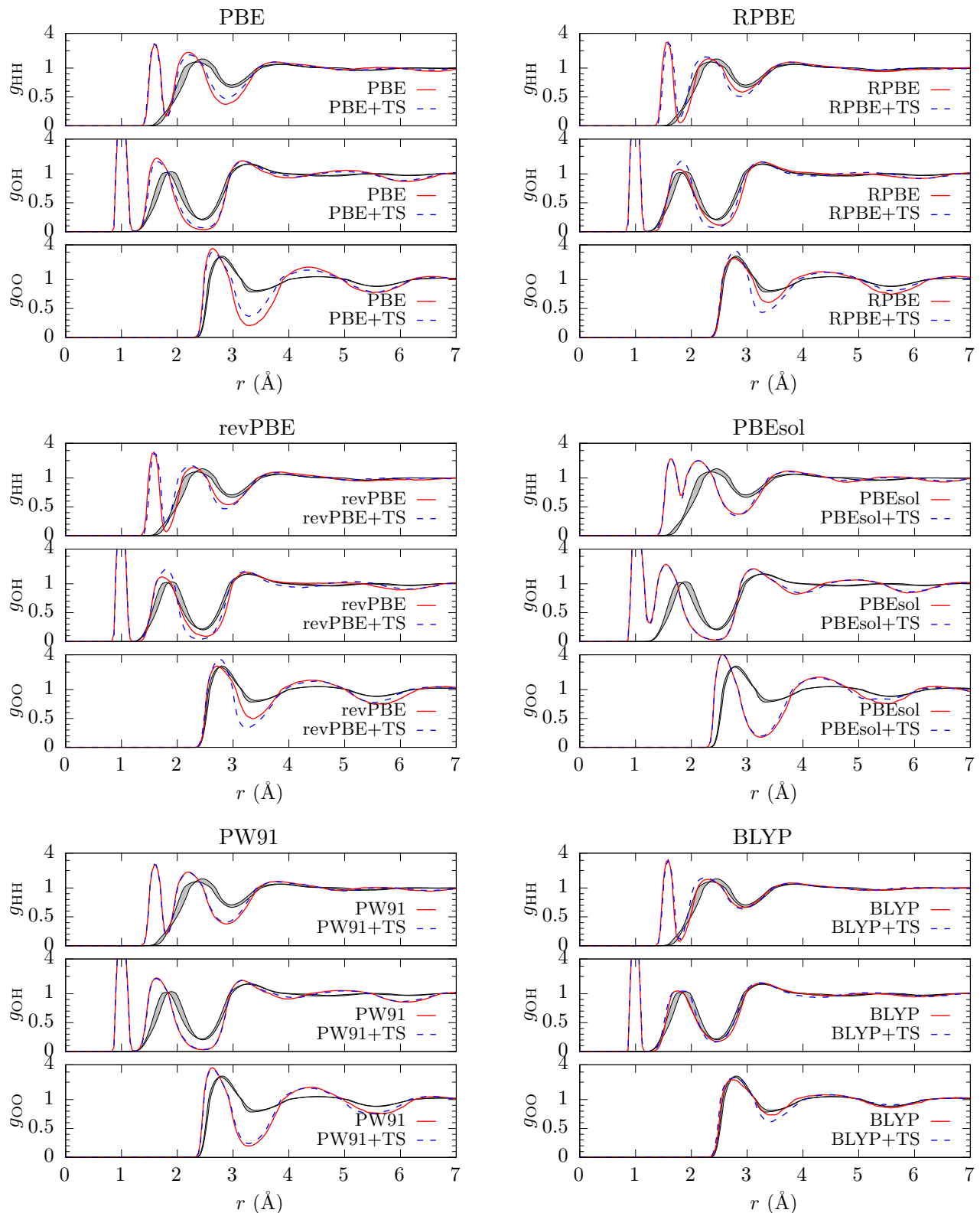


FIG. 4. Radial distribution functions calculated for the different GGAs studied in this paper and their dispersion-corrected counterparts ($T = 300$ K and $\rho = 1$ g/cm³). The shaded curves indicate experimental results at $T = 298$ K (including error margins) from Soper [33]. The peaks corresponding to intramolecular bonds are not shown by the experimental curves. The vertical axes are linear from 0 to 1 and logarithmic from 1 to 4. Numerical values for the positions of the different maxima and minima are given in Table III.

TABLE III. Position of the first two maxima and first two minima of the RFDs of liquid water depicted in Fig. 4.

XC functional	$r_{\max}^{(1)}$ (Å)	$g_{\max}^{(1)}$	$r_{\min}^{(1)}$ (Å)	$g_{\min}^{(1)}$	$r_{\max}^{(2)}$ (Å)	$g_{\max}^{(2)}$	$r_{\min}^{(2)}$ (Å)	$g_{\min}^{(2)}$
H-H RDF								
PBE	1.59	2.59	1.80	0.17	2.20	1.88	2.88	0.37
PBE+TS	1.59	2.64	1.80	0.14	2.23	1.69	2.85	0.48
RPBE	1.59	2.83	1.80	0.05	2.31	1.45	2.92	0.58
RPBE+TS	1.59	2.72	1.80	0.14	2.27	1.56	2.92	0.51
revPBE	1.59	2.80	1.80	0.07	2.27	1.52	2.92	0.54
revPBE+TS	1.59	2.66	1.80	0.17	2.23	1.64	2.85	0.47
PBEsol	1.62	2.14	1.80	0.70	2.13	2.00	2.85	0.37
PBEsol+TS	1.62	2.15	1.84	0.65	2.13	1.99	2.81	0.35
BLYP	1.59	3.07	1.80	0.08	2.27	1.41	2.92	0.66
BLYP+TS	1.59	2.94	1.80	0.11	2.23	1.49	2.92	0.64
PW91	1.59	2.47	1.80	0.20	2.20	1.89	2.88	0.37
PW91+TS	1.59	2.57	1.80	0.17	2.20	1.85	2.88	0.40
Experiment [33]	n/a	n/a	n/a	n/a	2.43	1.34	2.97	0.69
O-H RDF								
PBE	1.01	21.03	1.22	0.01	1.62	1.87	2.49	0.03
PBE+TS	1.01	20.88	1.22	0.01	1.66	1.62	2.49	0.07
RPBE	0.97	22.19	1.22	0.00	1.80	1.19	2.49	0.11
RPBE+TS	0.97	21.20	1.22	0.00	1.84	1.67	2.41	0.07
revPBE	0.97	21.44	1.26	0.00	1.73	1.32	2.52	0.09
revPBE+TS	1.01	21.26	1.22	0.00	1.80	1.81	2.41	0.04
PBEsol	1.01	18.00	1.26	0.33	1.55	2.18	2.49	0.03
PBEsol+TS	1.01	18.23	1.26	0.29	1.55	2.12	2.41	0.03
BLYP	0.97	24.51	1.22	0.00	1.77	1.12	2.45	0.17
BLYP+TS	0.97	23.55	1.22	0.00	1.84	1.11	2.41	0.16
PW91	1.01	20.72	1.22	0.01	1.62	1.88	2.49	0.03
PW91+TS	1.01	20.81	1.22	0.01	1.62	1.84	2.49	0.04
Experiment [33]	n/a	n/a	n/a	n/a	1.86	1.04	2.46	0.21
O-O RDF								
PBE	2.63	3.46	3.28	0.20	4.36	1.65	5.51	0.78
PBE+TS	2.63	3.05	3.28	0.37	4.32	1.46	5.58	0.78
RPBE	2.77	2.32	3.39	0.60	4.36	1.37	5.58	0.75
RPBE+TS	2.77	3.18	3.28	0.43	4.43	1.34	5.48	0.81
revPBE	2.70	2.56	3.35	0.49	4.40	1.45	5.69	0.74
revPBE+TS	2.77	3.35	3.24	0.33	4.50	1.40	5.51	0.78
PBEsol	2.56	4.13	3.24	0.18	4.29	1.64	5.55	0.75
PBEsol+TS	2.56	4.07	3.24	0.20	4.29	1.59	5.22	0.83
BLYP	2.74	2.20	3.42	0.73	4.36	1.22	5.58	0.85
BLYP+TS	2.81	2.38	3.42	0.62	4.36	1.19	5.40	0.90
PW91	2.63	3.56	3.28	0.20	4.43	1.64	5.66	0.76
PW91+TS	2.63	3.41	3.28	0.24	4.32	1.57	5.40	0.75
Experiment [33]	2.79	2.50	3.39	0.80	4.53	1.12	5.58	0.88

(PBEsol). Similarly, the self-diffusion coefficients are also underestimated by all the tested GGAs, varying between 10% (BLYP) and 83% (PBEsol). Unfortunately, it is likely that a fully satisfactory description of liquid water cannot be achieved with any XC functional at this level of theory, although BLYP offers very good performance.

With respect to dispersion corrections, it seems that the description of water is worsened by adding them for those functionals which require largest corrections, i.e., functionals which require small s_R values: RPBE, revPBE and BLYP. The description of liquid water is improved by including dispersion corrections for the other function-

als: PBE, PW91 and PBEsol.

IV. CONCLUSION

In conclusion, we have provided a list of optimal range parameters s_R for different XC functionals based on minimization of the MAE in the prediction of dispersion interactions of the S22 test set. These parameters allow computations of dispersion corrections to DFT based on the Tkatchenko-Scheffler method for the following GGAs: PBE, RPBE, revPBE, PBEsol, BLYP, AM05 and PW91. We have tested the effect of dispersion corrections on the description of liquid water offered by those functionals (except for AM05), finding no systematic improvement, i.e., the improvement is strongly functional-dependent. Based on our simulations, we recommend either BLYP for organic systems (due to its limitations to correctly describe metals), or RPBE more generally, as affordable options to carry out atomistic studies of systems includ-

ing water. When van der Waals interactions are expected to play a significant role, for instance in the presence of solvated organic molecules and adsorption phenomena, BLYP+TS and RPBE+TS can be good options, although the improvement over other GGAs is not so obvious as for the uncorrected cases. PBEsol was observed to perform particularly badly for liquid water, and we strongly advice against using PBEsol to simulate any system including an aqueous phase.

ACKNOWLEDGMENTS

Computational resources for this project were provided by CSC-IT Center for Science through the Taito supercluster. The author would like to thank Michael Walter for useful comments and email correspondence, as well as being an author of the GPAW implementation of the TS scheme.

Appendix: Code for s_R optimization

The following Python script can be used to optimize the s_R parameter for a given XC functional (or list of functionals) with the GPAW code:

```
# This code was adapted by M.A. Caro from Michael Walter's TS documentation on the GPAW website
from __future__ import print_function
from ase import Atoms
from ase.parallel import paropen
from ase.data.s22 import data,s22
from ase.calculators.vdwcorrection import vdWtkatchenko09pr1
from gpaw import GPAW, FermiDirac
from gpaw.cluster import Cluster
from gpaw.analyse.hirshfeld import HirshfeldPartitioning
from gpaw.analyse.vdwradii import vdWradii
import numpy as np

h = 0.18; box = 4.

sR_range = np.arange(0.88,1.02,0.02)
xc_list = ["PBE"]

for xc in xc_list:
    f = paropen('dispersion_energies_%s.dat' % xc, 'w')
    disp_en = {}
    for molecule in s22:
        disp_en[molecule] = []
        ss = Cluster(Atoms(data[molecule]['symbols'],
                           data[molecule]['positions']))
# Split interacting system into the separate molecules
        s1 = ss.find_connected(0)
        s2 = ss.find_connected(-1)
        assert(len(ss) == len(s1) + len(s2))
        c = GPAW(xc=xc, h=h, nbands=-6, occupations=FermiDirac(width=0.1))
        for s in [s1, s2, ss]:
            s.set_calculator(c)
            s.minimal_box(box, h=h)
            s.get_potential_energy()
            E = {}
            for sR in sR_range:
                cc = vdWtkatchenko09pr1(HirshfeldPartitioning(c),
```

```

                                vdWradii(s.get_chemical_symbols(), xc))
        cc.sR = sR
        s.set_calculator(cc)
        E[sR] = s.get_potential_energy()
        disp_en[molecule].append(E)
# Print
for sR in sR_range:
    print("# sR = %.3f" % sR, file=f)
    for molecule in s22:
        ref = data[molecule]["interaction energy CC"]
        E1 = disp_en[molecule][0][sR]
        E2 = disp_en[molecule][1][sR]
        E12 = disp_en[molecule][2][sR]
# Print molecule name, predicted interaction energy and reference CCSD(T) energy
    print("%s %.5f %.5f" % (molecule, E12 - E1 - E2, ref), file=f)
    print("", file=f)
f.close()

```

-
- [1] A. Tkatchenko and M. Scheffler, "Accurate molecular van der Waals interactions from ground-state electron density and free-atom reference data," *Phys. Rev. Lett.* **102**, 073005 (2009).
- [2] N. Marom, A. Tkatchenko, M. Rossi, V. V. Gobre, O. Hod, M. Scheffler, and L. Kronik, "Dispersion interactions with density-functional theory: benchmarking semiempirical and interatomic pairwise corrected density functionals," *J. Chem. Theory Comput.* **7**, 3944 (2011).
- [3] J. P. Perdew, K. Burke, and M. Ernzerhof, "Generalized gradient approximation made simple," *Phys. Rev. Lett.* **77**, 3865 (1996).
- [4] P. Jurečka, J. Černý, P. Hobza, and D. R. Salahub, "Density functional theory augmented with an empirical dispersion term. interaction energies and geometries of 80 noncovalent complexes compared with ab initio quantum mechanics calculations," *J. Comput. Chem.* **28**, 555 (2007).
- [5] P. Agrawal, A. Tkatchenko, and L. Kronik, "Pair-wise and many-body dispersive interactions coupled to an optimally tuned range-separated hybrid functional," *J. Chem. Theory Comput.* **9**, 3473 (2013).
- [6] B. Hammer, L. B. Hansen, and J. K. Nørskov, "Improved adsorption energetics within density-functional theory using revised Perdew-Burke-Ernzerhof functionals," *Phys. Rev. B* **59**, 7413 (1999).
- [7] Y. Zhang and W. Yang, "Comment on "Generalized gradient approximation made simple"," *Phys. Rev. Lett.* **80**, 890 (1998).
- [8] J. P. Perdew, A. Ruzsinszky, G. I. Csonka, O. A. Vydrov, G. E. Scuseria, L. A. Constantin, X. Zhou, and K. Burke, "Restoring the density-gradient expansion for exchange in solids and surfaces," *Phys. Rev. Lett.* **100**, 136406 (2008).
- [9] A. D. Becke, "Density-functional exchange-energy approximation with correct asymptotic behavior," *Phys. Rev. A* **38**, 3098 (1988).
- [10] C. Lee, W. Yang, and R. G. Parr, "Development of the Colle-Salvetti correlation-energy formula into a functional of the electron density," *Phys. Rev. B* **37**, 785 (1988).
- [11] Peter M. W. Gill, B. G. Johnson, J. A. Pople, and M. J. Frisch, "The performance of the Becke-Lee-Yang-Parr (B-LYP) density functional theory with various basis sets," *Chem. Phys. Lett.* **197**, 499 (1992).
- [12] R. Armiento and A. E. Mattsson, "Functional designed to include surface effects in self-consistent density functional theory," *Phys. Rev. B* **72**, 085108 (2005).
- [13] J. P. Perdew and Y. Wang, "Accurate and simple analytic representation of the electron-gas correlation energy," *Phys. Rev. B* **45**, 13244 (1992).
- [14] J. Enkovaara, C. Rostgaard, J. J. Mortensen, J. Chen, M. Dulak, L. Ferrighi, J. Gavnholt, C. Glinsvad, V. Haikola, H. A. Hansen, H. H. Kristoffersen, M. Kuisma, A. H. Larsen, L. Lehtovaara, M. Ljungberg, O. Lopez-Acevedo, P. G. Moses, J. Ojanen, T. Olsen, V. Petzold, N. A. Romero, J. Stausholm-Møller, M. Strange, G. A. Tritsarlis, M. Vanin, M. Walter, B. Hammer, H. Häkkinen, G. K. H. Madsen, R. M. Nieminen, J. K. Nørskov, M. Puska, T. T. Rantala, J. Schiøtz, K. S. Thygesen, and K. W. Jacobsen, "Electronic structure calculations with GPAW: a real-space implementation of the projector augmented-wave method," *J. Phys.: Condens. Matter* **22**, 253202 (2010).
- [15] A. Larsen, J. Mortensen, J. Blomqvist, I. Castelli, R. Christensen, M. Dulak, J. Friis, M. Groves, B. Hammer, C. Hargus, E. Hermes, P. Jennings, P. Jensen, J. Kermode, J. Kitchin, E. Kolsbjerg, J. Kubal, K. Kaasbjerg, S. Lysgaard, J. Maronsson, T. Maxson, T. Olsen, L. Pastewka, A. Peterson, C. Rostgaard, J. Schiøtz, O. Schütt, M. Strange, K. Thygesen, T. Vegge, L. Vilhelmsen, M. Walter, Z. Zeng, and K. W. Jacobsen, "The Atomic Simulation Environment – A Python library for working with atoms," *J. Phys.: Condens. Matter* (2017).
- [16] M. A. L. Marques, M. J. T. Oliveira, and T. Burnus, "LIBXC: A library of exchange and correlation functionals for density functional theory," *Comp. Phys. Comm.* **183**, 2272 (2012).
- [17] P. E. Blöchl, "Projector augmented-wave method," *Phys. Rev. B* **50**, 17953 (1994).
- [18] G. Kresse and D. Joubert, "From ultrasoft pseudopotentials to the projector augmented-wave method," *Phys.*

- Rev. B **59**, 1758 (1999).
- [19] M. J. Gillan, D. Alfè, and A. Michaelides, “Perspective: How good is DFT for water?” *J. Chem. Phys.* **144**, 130901 (2016).
- [20] I.-C. Lin, A. P. Seitsonen, I. Tavernelli, and U. Rothlisberger, “Structure and dynamics of liquid water from *ab initio* molecular dynamics: Comparison of BLYP, PBE, and revPBE density functionals with and without van der Waals corrections,” *J. Chem. Theory Comput.* **8**, 3902 (2012).
- [21] M. J. Abraham, T. Murtola, R. Schulz, S. Páll, J. C. Smith, B. Hess, and E. Lindahl, “GROMACS: High performance molecular simulations through multi-level parallelism from laptops to supercomputers,” *SoftwareX* **1**, 19 (2015).
- [22] H. J. C. Berendsen, J. R. Grigera, and T. P. Straatsma, “The missing term in effective pair potentials,” *J. Phys. Chem.* **91**, 6269 (1987).
- [23] W. L. Jorgensen and J. Tirado-Rives, “Potential energy functions for atomic-level simulations of water and organic and biomolecular systems,” *Proc. Natl. Acad. Sci. USA* **102**, 6665 (2005).
- [24] G. Kresse and J. Furthmüller, “Efficient iterative schemes for *ab initio* total-energy calculations using a plane-wave basis set,” *Phys. Rev. B* **54**, 11169 (1996).
- [25] M. A. Caro, T. Laurila, and O. Lopez-Acevedo, “Accurate schemes for calculation of thermodynamic properties of liquid mixtures from molecular dynamics simulations,” *J. Chem. Phys.* **145**, 244504 (2016).
- [26] M. A. Caro, O. Lopez-Acevedo, and T. Laurila, “Redox potentials from *ab initio* molecular dynamics and explicit entropy calculations: application to transition metals in aqueous solution,” under review.
- [27] P. H. Berens, D. H. J. Mackay, G. M. White, and K. R. Wilson, “Thermodynamics and quantum corrections from molecular dynamics for liquid water,” *J. Chem. Phys.* **79**, 2375 (1983).
- [28] S.-T. Lin, M. Blanco, and W. A. Goddard III, “The two-phase model for calculating thermodynamic properties of liquids from molecular dynamics: Validation for the phase diagram of Lennard-Jones fluids,” *J. Chem. Phys.* **119**, 11792 (2003).
- [29] S.-T. Lin, P. K. Maiti, and W. A. Goddard III, “Two-phase thermodynamic model for efficient and accurate absolute entropy of water from molecular dynamics simulations,” *J. Phys. Chem. B* **114**, 8191 (2010).
- [30] <http://dospt.org>.
- [31] M. Holz, S. R. Heil, and A. Sacco, “Temperature-dependent self-diffusion coefficients of water and six selected molecular liquids for calibration in accurate ^1H NMR PFG measurements,” *Phys. Chem. Chem. Phys.* **2**, 4740 (2000).
- [32] P. J. Linstrom and W. G. Mallard, eds., *NIST Chemistry WebBook, NIST Standard Reference Database Number 69* (2016).
- [33] A. K. Soper, “The radial distribution functions of water as derived from radiation total scattering experiments: is there anything we can say for sure?” *ISRN Physical Chemistry* **2013**, 279463 (2013).
- [34] A. Stroppa and G. Kresse, “The shortcomings of semi-local and hybrid functionals: what we can learn from surface science studies,” *New J. Phys.* **10**, 063020 (2008).